

PROSERVE: Unified Multi-Priority Request Scheduling for LLM Serving

Weizhe Huang¹, Tao Peng¹, Tongxuan Liu¹, Donghe Jin¹, Xianzhe Dong², Ke Zhang³

¹*JD.com* ²*USTC* ³*Unaffiliated*

Abstract

The widespread deployment of large language models (LLMs) for interactive applications necessitates serving systems that can handle thousands of concurrent requests with diverse Service Level Objective (SLO) requirements. A critical yet often overlooked dimension in this context is the *inherent priority difference among clients*; for instance, business-critical functions demand higher performance guarantees, as fulfilling such requests yields significantly greater business value. However, existing LLM serving schedulers fail to jointly optimize for both SLO attainment and client-level priorities.

To bridge this gap, we first *formalize multi-priority request scheduling as a service gain maximization problem*, where satisfying latency requirements for requests of different priorities contributes varying levels of gain. We then propose PROSERVE, a unified two-tier scheduling framework designed to maximize overall service gain. At the engine level, SlideBatching dynamically adapts batch formation and request ordering under varying load conditions, employing a sliding boundary mechanism to balance deadline-first and density-first strategies. At the service level, GoRouting performs gain-oriented and capability-aware dispatching across distributed instances, proactively reserving capacity for future high-priority or long requests. Extensive evaluation across four open-source datasets and a real-world industrial trace demonstrates that PROSERVE consistently outperforms state-of-the-art baselines, improving system gain by up to 35% and boosting SLO attainment by up to 52%.

1 Introduction

Large language models (LLMs) [10, 19, 41] have become foundational to a wide range of interactive applications, from chatbots [23] to autonomous agents [16]. As these LLM services are deployed at scale, they need to handle thousands of concurrent online requests with stringent and heterogeneous Service Level Objective (SLO) requirements [31, 46].

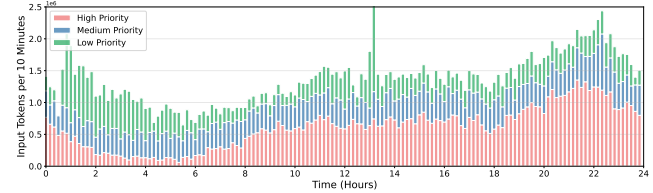


Figure 1: Workload trace of online requests with different priorities over one day from our real industrial dataset.

Beyond SLO diversity, a critical yet often neglected dimension is the **inherent priority difference among the clients themselves**. In real-world enterprise scenarios, for instance, business-critical functions demand higher performance guarantees than non-critical ones. To illustrate this, Figure 1 presents a real workload trace from our industrial dataset, which shows that requests of different priorities exhibit similar arrival patterns and load dynamics, yet satisfying a high-priority request typically yields significantly greater business value than satisfying a low-priority one. Therefore, an effective serving system must not only respect per-request SLOs, but also differentiate service based on client priority.

However, existing LLM serving schedulers fail to jointly account for both SLO diversity and client-level priorities. One line of work [5, 31, 42] addresses SLO heterogeneity by implicitly prioritizing requests with tighter deadlines, yet overlooks the inherent priority differences among the clients themselves. Another line of work [4, 30, 36] focuses on co-scheduling online and offline tasks, treating all online requests as uniformly high-priority (to be served with SLO guarantees) and offline ones as best-effort low-priority tasks without explicit latency requirements. This design makes such approaches inapplicable to our scenario, where both high- and low-priority requests carry their own latency requirements. Other works [27, 29] consider online client priority but inadequately account for SLO attainment. Llumnix [29] merely reserves static memory without providing explicit latency guarantees. Weighted VTC [27], inspired by Linux's Completely Fair Scheduler (CFS) [24], enforces token-based proportional fairness across

priority classes but cannot explicitly satisfy per-request latency target, which is yet critical in LLM serving. Consequently, there lacks a principled framework to simultaneously optimize for client priority and SLO attainment.

To bridge this gap, we first **formulate the multi-priority request scheduling problem as a service gain maximization task** (§2), where satisfying a high-priority¹ request’s latency requirement contributes substantially more service gain than low-priority one. We then jointly account for request priority and SLO requirements and propose a novel *Token-level Deadline-aware Gain (TDG)* function (§2) that quantifies the gain obtained from meeting the SLO of a specific-priority request. This formula explicitly captures the inherent differences of gain across different priority levels, while respecting the individual latency target for each request.

However, solving this problem introduces significant challenges in scheduler design. First, a fundamental trade-off exists between minimizing overall latency and favoring high-priority requests (§3.1). While naive policies like First-Come-First-Served (FCFS) [32] or recent SLO-aware schedulers [4, 5, 31] optimize overall latency and SLO attainment, they fail to differentiate request priorities, leading to insufficient service for high-priority requests. Conversely, an alternative strict-priority policy blindly prioritizes high-priority requests and starves low-priority ones. Both of them result in suboptimal total system gain. Second, we observe that the effectiveness of different batch scheduling policies varies significantly with load (§3.2). Under dynamic workloads shown in Figure 1, static scheduling policies may struggle to adapt across all load levels, limiting their effectiveness. Third, in distributed deployments, existing common global dispatchers (e.g., least-load) lack awareness of request priority and suffer from the *over-balancing* issue (§3.3). This may cause them to fail to accommodate future high-priority or long requests even when sufficient capacity is potentially available.

To address these challenges, we present PROSERVE (§4), a unified two-tier scheduling framework designed to maximize service gain from multi-priority requests. At the engine layer, we introduce SlideBatching (§4.2), a local batch scheduler that dynamically adapts its policy based on real-time load. It adaptively partitions the request queue into urgent and non-urgent subsets and applies tailored strategies. At the service layer, we design GoRouting (§4.3), a global request router that performs gain-oriented, capability-aware dispatching across distributed instances. It maintains awareness of local scheduler states and proactively reserves capacity for future high-priority or long requests. We evaluate PROSERVE against multiple common and state-of-the-art schedulers across four open-source datasets and one large-scale real-world industrial dataset. Extensive experiments demonstrate that PROSERVE consistently and significantly outperforms state-of-the-art baselines, improving system gain by up

¹Throughout this paper, we equate the request priority with the priority of the client from which it originates.

to 35% and boosting overall SLO attainment by up to 52%.

Our main contributions are summarized as follows:

- We formally define the multi-priority scheduling scenario and formulate it as a service gain maximization problem. We also propose a novel gain function TDG, which quantifies per-request gain while evaluating token delivery against deadlines.
- We introduce SlideBatching, a novel engine-level batch scheduler that dynamically adjusts request ordering strategies based on real-time load conditions.
- We design GoRouting, a service-level router that proactively monitors instance and request states and employs a gain-oriented, capability-aware routing policy.
- We demonstrate through extensive experiments that ProSched achieves superior and robust performance across diverse datasets and models.

2 Characterizing Request Priority and Service Objectives

Existing scheduling methods typically map request attributes (e.g., sequence length [9, 11, 13, 38], SLO constraints [5, 31, 42], online/offline type [4, 30, 36]) to execution priorities. However, they often fail to account for the inherent priority differences among the online clients themselves. Although all online requests come with their own SLO requirements, fulfilling the SLO for a high-priority request yields greater system gain than doing so for a low-priority one. To address this more general scenario, we formalize this *multi-priority request scheduling problem* as follows:

Objective Definition. *Let request r have a priority $p(r)$, where each priority level is associated with a priority weight $w_{p(r)}$ indicating its relative importance. If a request meets its latency target (e.g., SLOs), the system accrues the associated gain $f(r)$. The system’s objective is to maximize the total gain across the served request set R : $\max f(R) = \max \sum_{r \in R} f(r)$.*

The core issue then shifts to defining a proper per-request gain function $f(r)$ based on $w_{p(r)}$ and its own SLO _{r} .

Strawman Proposal 1: Weighted SLO Attainment. An intuitive idea is to weight the standard SLO attainment by priority:

$$f_W(r) = w_{p(r)} \cdot \mathbb{I}[TTFT_r \leq TTFT_{SLO}^r, TPOT_r \leq TPOT_{SLO}^r], \quad (1)$$

However, this formulation suffers from three key drawbacks: (1) *Discard-or-Postpone Trick*: Since gain is awarded only if both TTFT and TPOT SLOs are met, the system can immediately discard or indefinitely postpone any request whose TTFT SLO is deemed unattainable, as the gain for that request is already lost. This trick, while potentially improving the metric, significantly degrades user experience. (2) *Insensitivity to Per-Token Latency*: As an average metric, TPOT obscures the variability in per-token delivery times. For instance, a request with high initial latency but very fast subsequent tokens can

Gain Function	Vanilla SLO	Weighted SLO	Tempo [44]	TA-SLO	TDG(Ours)
Distinguishes Request Priority	✗	✓	✗	✓	✓
Aware of Per-Token Latency	✗	✗	✓	✓	✓
Distinguishes First/Decode Token Importance	✗	✗	✓	✓	✓
Robust to Discard/Postpone Trick	✗/✗	✗/✗	✓/✗	✓/✗	✓/✓

Table 1: The feature comparison of different per-request gain function.

yield the same TPOT as one with uniformly moderate latency. Consequently, both would attain the same gain $f_W(r)$, despite offering substantially different user experiences. (3) *Undifferentiated Importance of First and Decode Token*: In practice, TTFT and TPOT reflect different dimensions of service quality. TTFT measures the system’s initial responsiveness, whereas TPOT reflects the output fluency. A single, combined SLO condition fails to account for their differing impacts on the overall user experience.

Refined Proposal 2: Token-level Gain with TBT. To overcome these issues, we shift from the request-level SLO attainment to token-level gain function that aggregates the timely delivery of each output token. Inspired by prior work [44], our refined proposal is to replace TPOT with Time Between Tokens (TBT), leading to the initial Token-level Accumulated SLO (TA-SLO) formulation:

$$f_{TA-SLO}(r) = w_{p(r)} \cdot (w_p \cdot \mathbb{I}[TTFT_r < TTFT_{SLO}^r] + \sum_i w_d \cdot \mathbb{I}[TBT_{r,i} < TBT_{SLO}^r]), \quad (2)$$

where $TBT_{r,i} = t_{r,i} - t_{r,i-1}$ is the interval between consecutive tokens and $t_{r,i}$ denotes the output time of the i -th token of the request r . Here, w_p and w_d weight the importance of the first versus subsequent tokens.

However, *Postponed Decoding Trick* also persists in this definition. If a token is already detected to miss its TBT SLO, the system might intentionally delay its output to make the next token’s TBT easier to achieve. This distorts the gain calculation and stems from the negative monotonicity of the TBT metric: completing one token earlier can negatively impact the TBT SLO attainment of the next.

Our Final Proposal: Token-level Deadline-aware Gain (TDG). To overcome above limitations, we rethink a fundamental shift in perspective: the gain for a token is interpreted as a binary indicator of whether its output timing harms user experience. The individual token deadline represents the latest acceptable output time that does not degrade perceived quality. A token delivered after this deadline yields no gain (as it harms user experience), whereas earlier completion does not increase the gain for that specific token. Based on this insight, we replace TBT with the fixed deadline and introduce the Token-level Deadline-aware Gain (TDG):

$$f_{TDG}(r) = \sum_i w_r(i) \cdot \mathbb{I}[t_{r,i} < deadline_{r,i}],$$

$$deadline_{r,i} = TTFT_{SLO}^r + (i-1) \cdot TPOT_{SLO}^r, \quad (3)$$

$$w_r(i) = \begin{cases} w_p \cdot w_{p(r)} & , \text{if } i = 1 \\ w_d \cdot w_{p(r)} & , \text{otherwise} \end{cases}$$

where $w_r(i)$ is the gain for delivering the i -th token before its deadline. Weights w_p and w_d distinguish the importance of the first versus subsequent tokens, scaled by priority weight $w_{p(r)}$. This mapping can be adapted based on application-specific requirements.

A comprehensive comparison of TDG against other gain function is presented in Table 1. Furthermore, TDG establishes clear *monotonicity properties*: (1) *Positive Impact of Early Completion*. Although a token completed early gains no extra direct benefit, it increases the slack for subsequent tokens. Potential generation stalls caused by early output can be mitigated by the smoothing buffer mechanism [37] that can be seamlessly integrated into the front-end of LLM serving systems. This mechanism automatically caches sequentially output tokens and presents them at any predetermined intervals whenever tokens are available in the buffer². (2) *Negative Impact of Late Completion*. Because deadlines are fixed and independent, a late token directly reduces the available time for subsequent ones, creating a risk of deadline-miss propagation. This prevents the *Infinite-Postpone Trick* and discourages request discarding, as doing so forfeits all potential future gain.

3 Motivation

3.1 The Trade-off Between Overall Latency and Request Priority

Our objective gain function incorporates latency-related terms and the priority weights of request, indicating that both factors must be considered. However, an inherent trade-off exists

²In this work, we apply buffering [37] to all tokens, including the first token. If the first token can not be buffered, the deadline can be redefined as $deadline_{r,i} = \min\{TTFT_r, TTFT_{SLO}^r\} + (i-1) \cdot TPOT_{SLO}^r$, which can also align with current features.

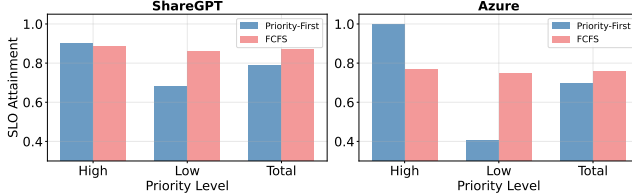


Figure 2: Latency of requests with different priorities in strict Priority-First and FCFS scheduling.

between minimizing overall latency and strictly favoring high-priority requests.

As shown in Figure 2, a strict priority scheduling policy always prioritizes high-priority requests. While this approach significantly improves SLO attainment for high-priority requests, the severe imbalance in computational resource allocation leads to poor overall latency guarantees for the system. Conversely, a mainstream First-Come-First-Served (FCFS) policy can achieve overall SLO attainment, but they fail to provide differentiated service quality between priority classes, resulting in overly similar SLO attainment rates for both high- and low-priority requests. In practice, however, guaranteeing lower latency for high-priority requests contributes more substantially to the total system gain. Thus, the key challenge we face is: how to design an effective scheduling algorithm that jointly balances overall latency and priority-based differentiation, thereby maximizing total system gain.

3.2 The Adaptive Deficit of Static Schedulers Under Dynamic Workloads

Online service workloads are volatile and unpredictable, fluctuating in intensity and priority distribution. For scheduler design, two key decisions must be made in each iteration: (1) *request admission order* and (2) *batch capacity*. Regarding the first, existing studies predominantly adopt fixed scheduling policies such as first-come-first-served (FCFS) [32], earliest-deadline-first (EDF) [4, 21], or shortest-job-first (SJF) [11, 38] and their variants, where FCFS can be viewed as a special case of EDF with uniform deadlines among requests. As for the second, existing inference engines such as vLLM [32] and xLLM [20] typically predefine a static token budget (e.g., `max_num_batched_tokens` in vLLM) or batch size limit (e.g., `max_num_seqs` in vLLM) and maintain it unchanged throughout scheduling. We show that static ordering policies lack adaptability to changing workloads, and their effectiveness depends on appropriate batch capacity.

Performance of Individual Scheduling Policies. Figures 3 and 4 compare scheduling policies under fixed batch size and token budget constraints. EDF outperforms SJF under low load, but drops sharply beyond a certain load threshold. This occurs because EDF optimistically allocates computational resources to the most urgent requests, assuming all can be completed. Under high load, this assumption fails as many

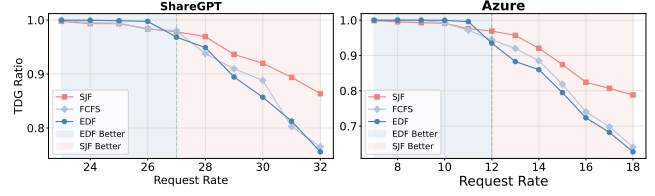


Figure 3: Performance of different request sorting strategies under the fixed token budget.

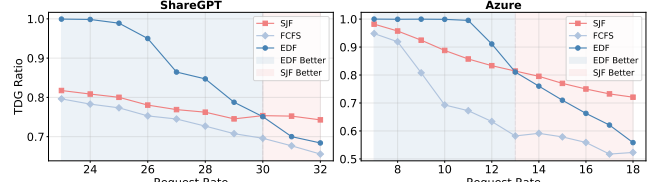


Figure 4: Performance of different request sorting strategies under the fixed batch size.

requests become urgent simultaneously, leading to widespread timeouts. Below, we provide an in-depth analysis of EDF and SJF under both low and high load conditions.

Figure 5 shows TTFT/TPOT distributions under low load. While both policies achieve high overall SLO attainment, SJF's bias toward short requests delays longer ones, causing some SLO violations. In contrast, EDF explicitly considers deadlines, preventing starvation and ensuring all requests meet their TTFT SLOs. Figure 6 tracks urgent and timed-out requests under high load. EDF causes a sudden accumulation of urgent requests during peak load, followed by a synchronized surge in timeouts. This vulnerability stems from its overly optimistic and averaged resource allocation strategy. In contrast, by prioritizing short requests, SJF avoids long-request blocking and massive delay propagation and maintaining stable counts of urgent and timed-out requests.

Impact of Batch Capacity. Figure 7 shows how different scheduling policies perform across load levels and batch capacity settings. As the token budget increases, EDF steadily improves and eventually stabilizes in SLO attainment. SJF initially improves but then degrades with further budget increases. FCFS behaves differently depending on load: under medium load, its SLO attainment first rises then falls; under high load, it resembles EDF's trend. These observations indicate that different scheduling policies have distinct preferences for batch capacity, and this preferred capacity can also fluctuate with changes in the system load. Consequently, a static and fixed batch capacity configuration appears insufficient to accommodate diverse scheduling strategies or adapt to real-world workload dynamics.

3.3 Limitations of Existing Global Schedulers

Unawareness of Local Scheduler and Request State. In a typical cluster deployment, an LLM service runs across

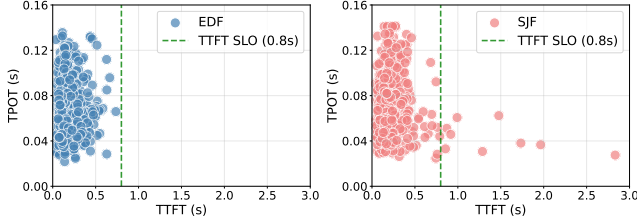


Figure 5: Distributions of TTFT and TPOT under different scheduling policies in low-load scenarios.

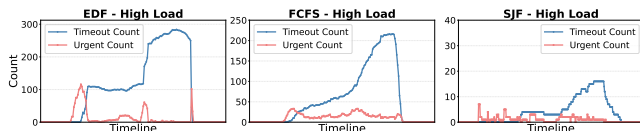


Figure 6: Timeline of urgent and timed-out requests under high load for different scheduling policies.

multiple instances. Existing global request dispatchers often completely ignore the local scheduling strategy and the state of ongoing requests. For instance, they may adopt naive policies such as round-robin or least-load, which rely only on coarse-grained, instance-level load indicators like request count. This oversight fails to account for the impact of diverse local scheduling strategies on overall system performance. Especially in multi-priority scheduling, a later-arriving high-priority request can gain local precedence (e.g., via queue jumping), affecting both its own gain and that of others, thereby influencing overall system performance. Consequently, an effective global scheduler should be sufficiently aware of the local scheduling policy, along with near-real-time instance and per-request states, to make informed dispatching decisions.

The Over-Balancing Issue. Existing global schedulers often use least-load dispatching [22, 32, 40] to balance workloads. However, given fluctuating request arrivals and varying lengths, strict load-balancing can be sub-optimal by hindering SLO attainment for future high-priority or long requests. As illustrated in Figure 8, when the longer request R2 arrives shortly after R1, a Min-Load policy dispatches R1 to the less-loaded Instance B to balance load instantly, leaving no instance with sufficient slack for R2’s SLO. Our SLO-aware strategy instead dispatches R1 to the moderately loaded Instance A, which still meets R1’s SLO while preserving capacity on Instance B for R2. Although R1’s TTFT increases slightly, both requests meet their deadlines. This demonstrates the need to move from pure load-balancing to a capacity-aware, SLO-driven policy that accounts for request length, deadline, and local scheduler behavior.

4 Design

The overall framework of PROSERVE is illustrated in Figure 9. PROSERVE consists of two primary components: SlideBatch-

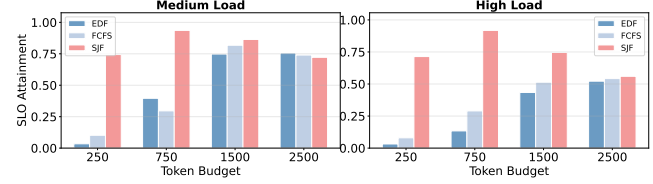


Figure 7: Performance of request scheduling policies under varying token budgets.

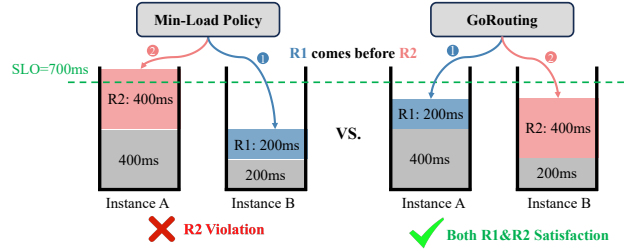


Figure 8: A toy example of the over-balancing issue.

ing at the engine layer and GoRouting at the service layer.

4.1 Batch Latency Estimator

The estimation of batch execution time is crucial for batch scheduling. The batch execution time can be decomposed into constant overhead (e.g., kernel launch and input/output processing), computation time, and memory access time. In general scenarios, a batch may contain both prefill and decode requests, where prefill requests are typically compute-intensive [1], dominated by linear and attention operations, whereas decode requests are typically memory-bound [46]. Hence, we formulate separate linear regression models for prefill and decode requests as follows:

$$T_{pd}(r) = \tilde{T}_{pd}(r) + t_c, \quad \tilde{T}_{pd}(r) = \begin{cases} \tilde{T}_p(r) & , r \text{ is prefill} \\ \tilde{T}_d(r) & , r \text{ is decode} \end{cases} \quad (4)$$

$$\tilde{T}_p(r) = a_p \cdot l_q(r)^2 + b_p \cdot l_q(r) \cdot l_{kv}(r) + c_p \cdot l_q(r) \quad (5)$$

$$\tilde{T}_d(r) = a_d \cdot l_{kv}(r) + b_d \cdot 1 \quad (6)$$

where $T_{pd}(r)$ denotes the estimated latency for request r including a constant overhead t_c , while $\tilde{T}_{pd}(r)$ represents the core computational latency estimate excluding this fixed overhead. $\{a_p, b_p, c_p, a_d, b_d\}$ are trainable parameters. $l_{kv}(r)$ denotes the KV cache length, and $l_q(r)$ is the number of tokens processed in the current forward pass. Then the execution time for a batch B can be estimated as:

$$T_{pd}(B) = T_{pd}(B_p \cup B_d) = \sum_{r \in B_p} \tilde{T}_p(r) + \sum_{r \in B_d} \tilde{T}_d(r) + t_c \quad (7)$$

We leverage offline-generated profiling batch data to train the models and similarly construct evaluation dataset. The evaluation results show that the Mean Absolute Percentage Error (MAPE) remains stable at approximately 4.5%.

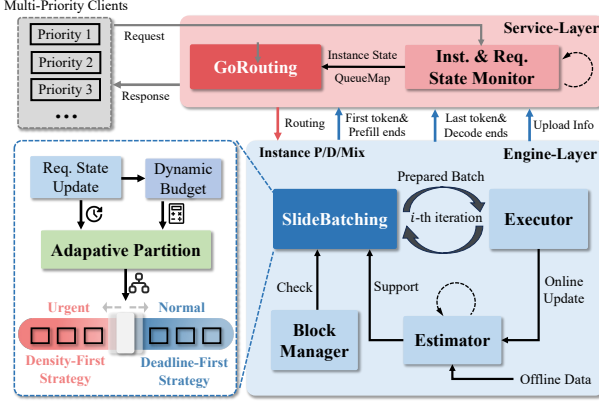


Figure 9: The overall framework of PROSERVE.

To further enhance runtime stability under fluctuating cluster loads, we perform online updates to the latency estimator. Specifically, we collect the actual execution time $T_{real}(B)$ and the estimated time $T_{pd}(B)$ for each batch B within a sliding time window. We then adjust a correction factor β_i in a momentum way: $\beta_{i+1} = \theta \cdot \beta_i + (1 - \theta) \cdot \text{mean}(\frac{T_{real}(B)}{T_{pd}(B)})$. The estimator is subsequently updated as $T_{pd}^{i+1} \leftarrow \beta_{i+1} \cdot T_{pd}^i$. This allows the estimator to continuously adapt to runtime variations while maintaining smoothing against transient noise.

4.2 Local Scheduler: SlideBatching

The key of the batch scheduling policy lies in determining the batch capacity and the order of requests to admit. Our core design principle is: *when possible, satisfy all request deadlines to capture full system gain; when current load cannot meet the deadlines of all requests, prioritize high-priority requests to maximize overall gain*. To this end, we propose the SlideBatching algorithm that effectively balances request latency and priority.

Algorithm. While batch capacity is typically defined by token budget or batch size, thanks to the latency estimator introduced in §4.1, we can directly transform token- or sequence-level budgets into a time-level *latency budget*, comparable to request deadlines. Algorithm 1 first sets this budget to the smallest remaining deadline among queued requests (line 6), ensuring no request misses its deadline in the current batch. To avoid overly small batches under high load, a lower bound η is enforced (line 7). The core of the algorithm is the request ordering strategy in line 13: we prioritize URGENT requests, and within the URGENT group, we schedule requests in descending order of their *density* (line 5). The remaining requests are scheduled in ascending order of their remaining time to deadline ($r.\text{remain}$). The numbers of URGENT and NORMAL requests vary dynamically with the queue load, and the boundary between them “slides” accordingly.

Adaptive Urgency Partition. The algorithm dynamically diagnoses request urgency (lines 9–13) to prioritize URGENT

Algorithm 1 SlideBatching Algorithm

Input: the request queue Q

Output: prepared batch of requests B .

```

1:  $t_{\text{exec}}, t_{\min} \leftarrow 0, \infty$ 
2: for  $r$  in  $Q$  do ▷ Update request metric
3:    $r.\text{exec} \leftarrow \tilde{T}_{pd}(r)$ 
4:    $r.\text{remain} \leftarrow \text{deadline}_r, r.\text{output\_len} + 1 - r.\text{elapsed\_time}$ 
5:    $r.\text{density} \leftarrow \frac{w_r(r.\text{output\_len} + 1)}{r.\text{exec}}$ 
6:    $t_{\min} \leftarrow \min(t_{\min}, r.\text{remain})$ 
7:    $t_{\text{budget}} \leftarrow \max(t_{\min}, \eta)$ 
8: for  $r$  in  $Q$  do ▷ Determine requests' urgency
9:   if  $r.\text{remain} < \gamma \cdot \phi(r, Q)$  then
10:     $r.\text{state} \leftarrow \text{URGENT}$ 
11:   else
12:     $r.\text{state} \leftarrow \text{NORMAL}$ 
13: Sort  $Q$  first by  $r.\text{state}$ , then sort URGENT requests in descending order of  $r.\text{density}$  and sort NORMAL requests in ascending order of  $r.\text{remain}$ .
14:  $t_{\text{batch}} \leftarrow t_c$ 
15: while  $Q$  and  $t_{\text{batch}} < t_{\text{budget}}$  and memory is enough do
16:    $r \leftarrow Q.\text{pop}()$ 
17:    $t_{\text{batch}} \leftarrow t_{\text{batch}} + \text{GETMAXCHUNK}(r, t_{\text{budget}} - t_{\text{batch}})$ 
18:    $B \leftarrow B \cup \{r\}$ 
19: return  $B$ 

```

requests at risk of missing deadlines. A request is *URGENT* if it is likely to miss its deadline under current load. This requires a load-judgment function $\phi(r, Q)$ that compares estimated completion time against $r.\text{remain}$. Since a request excluded from the current batch might still be served later, ϕ should estimate whether it can be completed in any future batch.

In the *PD co-located setting*, we approximate the latency budget of future batches using the current t_{budget} . This is reasonable because, when the queue cannot be fully served, the algorithm tends to saturate t_{budget} via ChunkedPrefill (line 18). Consequently, each batch contains requests that either just meet or miss deadlines. If such a request is still running (implying it has entered the decoding phase), the minimum remaining time to deadline in the next batch will be shorter than its TPOT_{SLO} (which is relatively small). Given the lower bound η , t_{budget} fluctuates within $[\eta, \max(\text{TPOT}_{\text{SLO}})]$, so successive budgets remain relatively stable. We then consider two alternative implementations of the load-judgment function ϕ .

(1) **Request-Agnostic Aggressive Estimation.** We adopt a worst-case perspective by statically placing every request at the end of the *NORMAL* queue and evaluating whether it would miss its deadline under this pessimistic assumption. Consequently, more requests are classified as *URGENT*. The corresponding function ϕ_a is formulated as:

$$\phi_a(Q) = \frac{t_{\text{budget}}}{t_{\text{budget}} - t_c} \sum_{r \in Q} r.\text{exec} \quad (8)$$

where t_c denotes the constant per-batch overhead introduced in §4.1 and the term $\frac{\sum_{r \in Q} r.\text{exec}}{t_{\text{budget}} - t_c}$ represents the number of batch steps required to process the entire request queue Q .

(2) **Request-Specific Conservative Estimation.** We dynamically determines a request's position in the queue. All requests are assumed to reside in the NORMAL queue, which is sorted in ascending order of remaining time $r.\text{remain}$. This ordering reflects the expected batch-admission sequence. Denoting $\text{req}.\text{index}$ as the position of request req in this sorted queue Q , the corresponding function ϕ_c is formulated as:

$$\phi_c(\text{req}, Q) = \frac{t_{\text{budget}}}{t_{\text{budget}} - t_c} \sum_{i=0}^{\text{req}.\text{index}} Q[i].\text{exec} \quad (9)$$

For the *PD disaggregation setting*, we only schedule the prefetch-only instance, as decode requests are interference-free and typically batched together [33]. Given that prefetch execution times are relatively long, we adopt a worst-case estimation which leads to a simplified load-judgment function: $\phi_p(r, Q) = \sum_{r \in Q} r.\text{exec} + |Q| \cdot t_c$, where each batch is assumed to contain only one request.

Additionally, we introduce an *aggressiveness coefficient* γ (line 10), which can be adjusted manually. A larger γ shifts more requests towards the URGENT side, favoring density-first scheduling pessimistically to capture short-term gain, whereas a smaller γ shifts more requests toward the NORMAL side, favoring deadline-first scheduling optimistically in pursuit of long-term gain.

Analysis. The algorithm's behavior adapts to the system's actual load through its sliding boundary mechanism. (1) **Low Load:** The latency budget accommodates all queued requests, rendering the specific ordering strategy negligible in its impact. (2) **Medium load:** A subset of requests is classified as URGENT, but the batch capacity is still sufficient to accommodate all urgent requests along with some normal ones. The scheduling policy remains predominantly deadline-first, prioritizing requests with the earliest deadlines. (3) **High load:** The number of urgent requests increases sharply, exceeding the batch capacity, which means that only a subset of urgent requests can be admitted into the current batch. As long as the minimum remaining time among requests is greater than the threshold η , each request selected for the batch is expected to meet its deadline and yield its gain. In this context, each local batch formation can be modeled as a *fractional knapsack problem*: the latency budget t_{budget} serves as the knapsack capacity, the estimated execution time $r.\text{exec}$ as the item size and the token-level gain $w_r(i)$ as the item value. Supported by ChunkedPrefill, requests can be approximately treated as divisible items, making our density-first greedy strategy optimal for this classic problem formulation. (4) **Very high load:** Nearly all requests may be classified as urgent. In this extreme case, the scheduling policy converges to a pure density-first strategy, focusing solely on maximizing immediate gain per forward time.

Algorithm 2 GoRouting Algorithm for PD Disagg.

Input: prefill instance pool P , decode instance pool D , request req , request queues PrefillQueueMap maintained for instances

Output: Selected instance pair $(p_{\text{inst}}, d_{\text{inst}})$

```

1:  $\Delta_{\text{max}} \leftarrow -\infty$ 
2: for  $p$  in  $P$  do  $\triangleright$  Estimate each instance's gain
3:    $Q \leftarrow \text{PrefillQueueMap}[p]$ 
4:    $\text{pre\_gain} \leftarrow \text{ESTIMATEGAIN}(Q)$ 
5:    $\text{post\_gain} \leftarrow \text{ESTIMATEGAIN}(Q \cup \{\text{req}\})$ 
      $\triangleright$  Based on specific local scheduler
6:    $\Delta_p = \text{post\_gain} - \text{pre\_gain}$ 
7:    $\Delta_{\text{max}} \leftarrow \max(\Delta_{\text{max}}, \Delta_p)$ 
8:  $C \leftarrow \{p \in P \mid \Delta_p \geq \alpha \cdot \Delta_{\text{max}}\}$   $\triangleright$  Candidates
9: if  $\Delta_{\text{max}} > 0$  then
10:   $L \leftarrow \{p \in C \mid \text{ESTIMATEEXEC}(p) < \mu \cdot \text{TTFT}_{\text{SLO}}\}$ 
11:   $H \leftarrow \{p \in C \mid \text{ESTIMATEEXEC}(p, \text{req}) > \lambda \cdot \text{TTFT}_{\text{SLO}}\}$ 
12:  if  $L \neq \emptyset$  then
13:     $p_{\text{inst}} \leftarrow \arg \min_{p \in L} \text{ESTIMATEEXEC}(p)$ 
14:  else if  $C - H \neq \emptyset$  then
15:     $p_{\text{inst}} \leftarrow \arg \max_{p \in C - H} \text{ESTIMATEEXEC}(p)$ 
16:  else
17:     $p_{\text{inst}} \leftarrow \arg \min_{p \in C} \text{ESTIMATEEXEC}(p)$ 
18:  else
19:     $p_{\text{inst}} \leftarrow \text{RANDOMSELECT}(P)$   $\triangleright$  Fallback
20:  $d_{\text{inst}} \leftarrow \text{LOADBALANCE}(D)$ 
21: return  $(p_{\text{inst}}, d_{\text{inst}})$ 

```

4.3 Global Scheduler: GoRouting

GoRouting is designed to support both PD co-located and PD disaggregated [46] deployments, which are widely used in modern engines (e.g., vLLM [32], xLLM [20]).

Instance State Monitoring and Update. To accurately track the load of local instances while minimizing communication overhead between the local and global schedulers, the global scheduler maintains a real-time list of prefetch requests running on each instance, denoted as PrefillQueueMap .

In the **PD disaggregated** setting, when the global scheduler dispatches a request r to a prefill instance p , it immediately updates $\text{PrefillQueueMap}[p].\text{add}(r)$. Once a request finishes on instance p , an asynchronous completion signal is sent to the global scheduler, triggering $\text{PrefillQueueMap}[p].\text{remove}(r)$. For decode instances, the global scheduler simply tracks the number of free blocks reported by each local instance.

In the **PD co-located** setting, we similarly maintain the prefetch request list PrefillQueueMap . However, maintaining the full per-request decode state in the global scheduler would incur substantial communication overhead. Because each decode execution time is relatively short and stable, we instead maintain a counter n_d that records the number of requests

currently in the decode phase on each instance. Specifically, when the service returns the first token of a request to the front-end, it simultaneously updates *PrefillQueueMap* and increments n_d ; when the request completes, n_d is decremented.

Moreover, relying solely on *PrefillQueueMap* can lead to information lag: the scheduler may dispatch a request based on the current queue state, while a prefill request on some instance may finish imminently. Since prefill execution times are typically long, such lag can significantly degrade scheduling accuracy. To obtain a more precise view, the global scheduler also records a timestamp ts_p for each update to *PrefillQueueMap*[p]. When estimating the execution time on instance p , the elapsed time $ts_{curr} - ts_p$ is subtracted from the predicted execution time to compensate for this delay.

Instance Selection in PD Disaggregated Settings. The request-dispatching algorithm is detailed in Alg. 2. For each instance p , the ESTIMATEGAIN procedure evaluates whether the incoming request can meet its TTFT_SLO on p and how its admission would affect other requests already in the queue (line 2-5). This yields a predicted gain before dispatching (pre_gain) and after dispatching (post_gain). The implementation of ESTIMATEGAIN depends on the specific local scheduler running on this prefill instance. We adopt the similar conservative estimation strategy described in §4.2 and employ ϕ_p to estimate the total execution latency. The corresponding gain is then derived from this estimation.

The incremental gain for instance p is $\Delta_p = \text{post_gain} - \text{pre_gain}$, and the maximum gain across all instances is $\Delta_{\max} = \max_{p \in P} \Delta_p$. A positive Δ_{\max} indicates that at least one instance can satisfy the request’s TTFT SLO. If the request cannot meet its SLO on any instance, Δ_{\max} will be non-positive, because adding the request does not shorten other requests’ latencies and instead tends to increase them, thereby reducing the overall gain. Since multiple instances may yield similarly high gains (e.g., all requests can be completed before its within its SLO), we then introduce a threshold α to obtain a candidate set C of instances whose gains are close to Δ_{\max} (line 17). Every instance in C is capable of satisfying the request’s SLO.

As noted in §3.3, an overly balanced dispatching strategy struggles to accommodate fluctuating request lengths, which may cause subsequent long requests to miss their SLOs. To this end, we employ a dual-threshold capability-aware dispatching policy (lines 18–29). Let L denote the subset of C with relatively light load, and H the subset with relatively high load; these are defined by an upper threshold λ and a lower threshold μ . The final selection proceeds as follows:

- (1) If $L \neq \emptyset$, we dispatch the request to the most idle instance in L to prevent under-utilization.
- (2) If $C \setminus H = \emptyset$ (i.e., all candidates are heavily loaded), we fall back to a load-balancing strategy, selecting the least-loaded instance in C to avoid pushing any instance into overload.
- (3) Otherwise, we remove the high-loaded instances (H) from C and select the instance with the relatively heaviest load

among the remaining candidates. Although this may increase the TTFT of the dispatched request, the properties of C guarantee that the request can still meet its TTFT SLO and obtain its gain, while reserving capacity on lighter-loaded instances for future potentially high-priority and long requests.

For decode instance, the execution of decode requests is not interfered with by prefill [46]. The main constraint for decode instances is typically memory bound. We select the decode instance with the largest number of free blocks.

Instance Selection in PD Co-located Settings. For request dispatching under PD co-location, the fact that a request remains on the same instance for both prefill and decode phases significantly complicates the gain calculation. For simplicity, we assume that decode requests are always included in the batch (since their execution time is short and TPOT is typically small) and that they always meet their deadlines. We then consider only the gain contributed by prefill requests, which allows us to reuse Alg. 2 almost seamlessly.

The adjustment is that when estimating the execution time for prefill on the instance, we add the estimated decode time $n_d \cdot b_d$, where b_d is the average decode time. Furthermore, in SlideBatching, the ordering of requests in the queue changes dynamically with the load. To avoid an overly optimistic estimate of how admitting a new request interferes with existing ones, we adopt a conservative strategy and implement the ESTIMATEGAIN based on ϕ_a (Eq. 8). In this context, the estimated t_{budget} is set to the minimum of the smallest remaining time among prefill requests and the TPOT SLO.

4.4 Implementation

PROSERVE is implemented on top of the recently open-sourced, high-performance LLM inference system xLLM [40], which is written entirely in C++. In total, we added approximately 4K lines of C++ code for the scheduler, 2K lines of Python for the client and evaluation modules, and 1K lines of shell scripts for automation. Based on preliminary results showing a slight performance advantage of ϕ_a over ϕ_c in SlideBatching, ϕ_a is adopted as the load-judgment function for all reported results under the PD-colocated setting.

5 Evaluation

5.1 Experimental Setup

Datasets and Workloads. We evaluate our method on four open-source datasets: ShareGPT [26], Azure [28], BurstGPT [35], and QwenTrace [34]. For datasets with real timestamps (Azure, QwenTrace, and BurstGPT), we adopt a commonly used scaling method [25, 35, 39]. This approach expands the timestamps according to a pre-defined overall request rate, and then replays the requests following the scaled intervals. For datasets lacking real timestamps (ShareGPT),

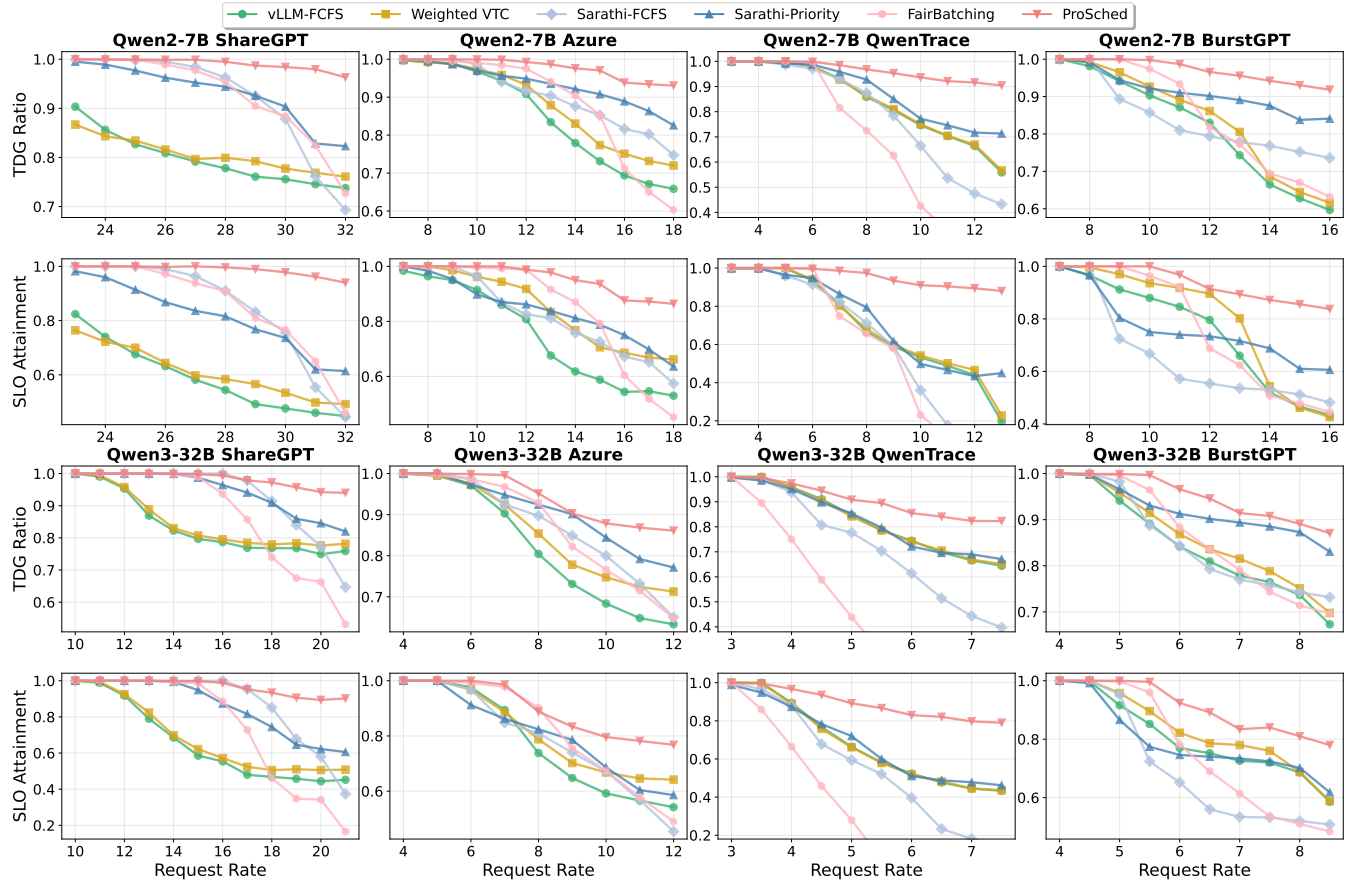


Figure 10: Performance of different methods across different datasets and models under the single-node setting.

We employ a Poisson distribution to simulate the request arrival pattern. Additionally, we also include our proprietary industrial dataset, which will be described in §5.7.

Testbd and Models. We deploy PROSERVE based on the recent open-source xLLM [20] inference engine framework with the server equipped with 16 Ascend 910B NPUs, 96 physical CPU cores, and 2 TB of RAM. And we select the Qwen2-7B [2] and Qwen3-32B [41] models for our experiments.

Baselines. We compare PROSERVE against the following batch scheduling algorithms:

- **vLLM-FCFS** [32]: The default scheduling algorithm in vLLM. It prioritizes prefill requests and employs FCFS.
- **Weighted VTC** [27]: A variant of the VTC algorithm. VTC is designed for fairness in LLM serving, aiming to equalize the number of tokens served across clients. Building upon this, Weighted VTC assigns different priority weights (analogous to the *nice* values in Linux) to clients, ensuring the ratio of tokens processed approximates the ratio of assigned priority weights.
- **Sarathi-FCFS** [1]: The scheduler in Sarathi-Serve, which employs chunked prefill. It prioritizes decode requests and uses FCFS within each request type. It uses profiled token budget based on TBT.

- **Sarathi-Priority**: A priority-based extension of above Sarathi-FCFS. When ordering requests, it strictly prioritizes decode requests first, followed by those with higher priority, and finally, those that arrived earlier.
- **FairBatching** [21]: A recently proposed scheduling algorithm that employs an enhanced EDF policy. It schedules requests by prioritizing decode sequences nearing their deadlines, followed by prefill sequences, and finally the remaining decode requests.

In multi-node experiments, we use the widely adopted Min-Load strategy as the global scheduler baseline, which dispatches each request to the least-loaded instance. For a fair comparison, all schedulers including our proposed methods, are uniformly implemented within the xLLM [20] framework.

Metrics. We select the TDG introduced in §2 as gain function to quantify service gain for requests of different priorities. We further define the system-level gain metrics as $\text{TDG_Ratio} = \frac{\sum_r f_{TDG}(r)}{\text{Ideal_Gain}}$ and $\text{Miss_TDG_Ratio} = \frac{\text{Ideal_Gain} - \sum_r f_{TDG}(r)}{\text{Ideal_Gain}}$, which respectively represent the proportion of captured gain and the proportion of lost gain relative to the total achievable gain. In addition, we report the SLO attainment ratio, a standard metric widely adopted in recent work [8, 14, 31, 39, 42]. A request is considered to have met

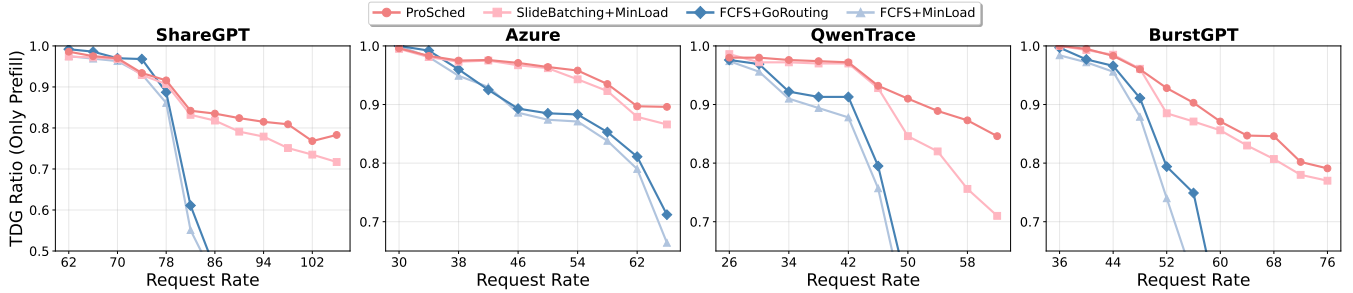


Figure 11: Performance of different methods across datasets in PD disaggregated multi-node deployment.

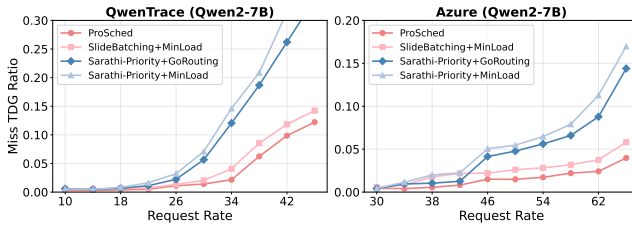


Figure 12: Performance of different methods across datasets in PD co-located multi-node deployment.

its SLO only when both its observed TTFT and TPOT are strictly less than the preset SLO thresholds.

Details. To simulate a multi-priority scenario, each request in the dataset is randomly designated as high or low priority with a 50% probability. In our experiments, the priority weights are fixed at 2 and 1 for high- and low-priority requests, respectively. An analysis of how different priority weight configurations affect our method is provided in §5.6. The ratio between the first-token weight and the decode-token weight in TDG is configured based on the average ratio of input to output length from the dataset.

5.2 Main Results

Single-Node Performance. Figure 10 compares batch scheduling strategies under single-node PD co-location. Figure 10 shows that PROSERVE consistently outperforms all baselines in both TDG and SLO attainment across all tested datasets and models, demonstrating its superior ability to schedule multi-priority requests under varying loads. Second, deadline-first based strategies (e.g., FairBatching and Sarathi-FCFS) perform well under low load, matching PROSERVE in system gain. However, their performance degrades sharply at higher request rates, falling below even vLLM-FCFS and Weighted VTC. This confirms that while such strategies work under light load, they become suboptimal under contention and lead to widespread deadline misses, which aligns with our analysis in §3.2. Third, although Sarathi-Priority and Weighted-VTC consider priority, each has critical flaws. Sarathi-Priority’s strict prioritization starves low-priority requests, hurting overall gain. Weighted VTC focuses

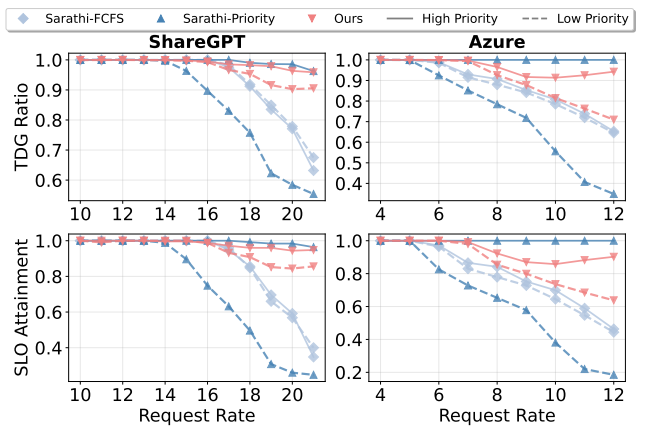


Figure 13: Performance for different priority requests under various scheduling strategies using Qwen3-32B.

only on token-based fairness and ignores SLO constraints, resulting in poor TDG and SLO attainment.

Multi-Node Performance. Since the PD-disaggregated setting inherently favors decode requests, the TDG for decode tokens is almost always satisfied in our experiments. we report only the first-token TDG. First, as shown in Figure 11, GoRouting enhances various local schedulers. While not always selecting the least-loaded node, its SLO-aware dispatch matches minimum-load performance under light load. At higher loads, it reserves capacity for future long requests, improving overall TDG. Second, the improvement with SlideBatching exceeds that with GoRouting, as GoRouting’s effectiveness depends on specific traffic patterns, while SlideBatching adapts better to diverse request arrivals. Moreover, results are consistent under PD co-located multi-node deployment (Figure 12), confirming the effectiveness of both SlideBatching and GoRouting in this scenario.

5.3 Performance of Different Priorities

To demonstrate our method’s ability to balance latency guarantees for high-priority requests with overall system performance, Figure 13 compares TDG and SLO satisfaction across priority levels. PROSERVE achieves slightly better TDG and SLO satisfaction for high-priority over low-priority requests,

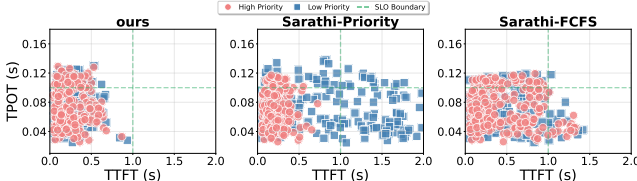


Figure 14: TTFT and TPOT distributions for different priority requests under various scheduling strategies.

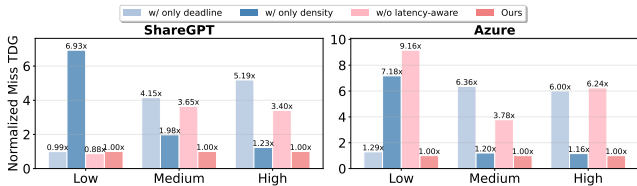


Figure 15: Performance of ablation study for SlideBatching.

maintaining a desirable priority ordering while keeping both at high absolute levels—consistently outperforming Sarathi-FCFS. In contrast, Sarathi-Priority strictly prioritizes high-priority requests, causing severe performance degradation and starvation for low-priority ones, which ultimately lowers overall system gain compared to PROSERVE. Figure 14 further compares TTFT and TPOT distributions. PROSERVE achieves a balanced latency distribution across priorities, with minimal disparity between high- and low-priority requests. Sarathi-Priority, however, exhibits significantly larger TTFT for low-priority requests, resulting in many SLO violations. Besides, while Sarathi’s decode-prioritized strategy yields slightly better TPOT, it causes substantial TTFT timeouts.

5.4 Ablation Study

To validate the effectiveness of the individual modules in PROSERVE, we conduct an ablation study. The configurations *w/ only deadline* and *w/ only density* represent simplified versions where the Adaptive Urgency Partition module is removed, retaining only the deadline-prioritized strategy or the density-prioritized strategy, respectively. *w/o latency-aware* denotes disabling the latency estimator that predicts request latency and restricts batch capability. As shown in Figure 15, removing any of these modules leads to performance degradation, demonstrating the necessity of our proposed components. Furthermore, *w/ only deadline* outperforms *w/ only density* under lower load conditions, whereas the opposite trend is observed under higher load. This behavior aligns with the insights discussed in §3.2.

5.5 Timeline Analysis

Figure 16 illustrates the timeline of TDG obtained per second by Sarathi-FCFS and PROSERVE under relatively high load on the Azure dataset. Sarathi-FCFS initially achieves

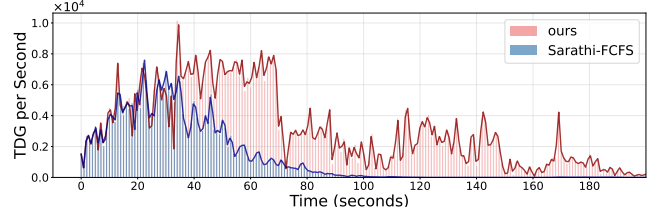


Figure 16: The request servicing timelines of PROSERVE and baseline methods during a representative service session.

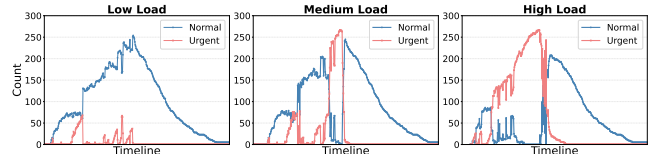


Figure 17: The urgent and normal request distribution timelines of PROSERVE under different load (request rate).

TDG under low-load conditions; however, as the cumulative load increases, its FCFS-based scheduling can lead to widespread request timeouts, causing TDG to approach zero in subsequent service intervals. In contrast, PROSERVE can adaptively respond to load variations. It employs an approximately deadline-first strategy during low-load periods, achieving higher TDG than Sarathi-FCFS. More importantly, upon detecting high cumulative load conditions, PROSERVE dynamically switches to its high-load scheduling mode, prioritizing high-priority and relatively short requests to maintain sustained TDG acquisition throughout the service period. Figure 17 further illustrates the timeline of urgent and normal request counts partitioned by SlideBatching under different loads. It can be observed that our method adaptively adjusts the number of each type in response to load fluctuations.

5.6 Priority Weight Scaling

Figure 18 illustrates the SLO satisfaction rates of different priority requests and the overall system in PROSERVE under various load conditions as the priority weight increases. Several key observations can be drawn. First, across all load levels, the SLO satisfaction rate for high-priority requests shows a significant upward trend as the priority weight increases, while that of low-priority requests gradually declines. Notably, the overall SLO satisfaction rate remains stable, indicating that our method effectively balances the latency requirements between high- and low-priority requests. Second, under high load conditions, the SLO satisfaction rate of high-priority requests exhibits more pronounced improvement with increasing priority weight. This demonstrates that our method adapts to workload intensity by more aggressively protecting high-priority requests to maintain overall service gain under high load, while striving to guarantee latency for all requests under low-to-medium load. Third, as the priority weight grows, the SLO satisfaction rate of high-priority requests in PROS-

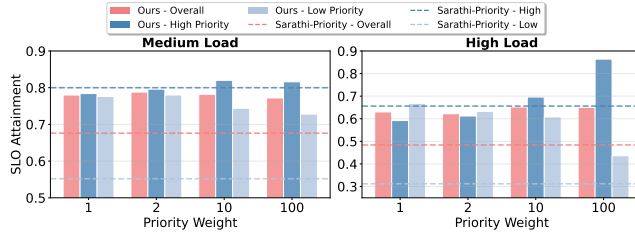


Figure 18: Effects of priority weight scaling on multi-priority request performance in PROSERVE.

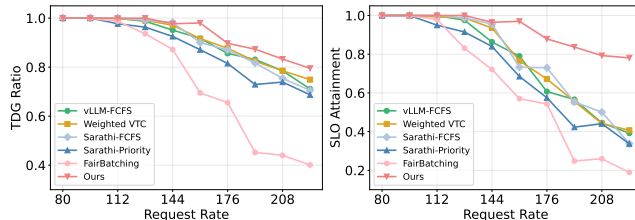


Figure 19: Performance of different methods on a large-scale cluster using a proprietary industrial dataset.

ERVE initially lags behind Sarathi-Priority but eventually surpasses it. Moreover, our method consistently achieves better overall SLO satisfaction and low-priority request satisfaction than Sarathi-Priority, which strictly prioritizes high-priority requests. These results confirm the superiority of our approach in dynamically meeting the latency requirements of different priority levels.

5.7 Large-Scale Cluster Experiments

We conduct experiments using our proprietary industrial dataset (the distribution is shown in Figure 1). The priority weights for different priorities are assigned according to their actual business value in our production environment. The experiments run on a cluster of 8 servers, each equipped with 16 Ascend 910B NPUs. We deploy 32 instances of the Qwen3-32B model [41]. As shown in Figure 19, our method consistently outperforms all baseline methods even at this large scale and on the real-world industrial workload.

6 Related Work

LLM Serving. Existing works have optimized LLM serving systems from various perspectives, such as kernel optimization [6, 7, 15, 43], prefix cache [45] and KV cache management [17, 18, 25]. These system-level optimizations are orthogonal to our approach and can be seamlessly integrated. For LLM scheduling, Sarathi-Serve [1] employs chunked prefill and a stall-free batching strategy to mitigate the interference caused by prefill requests on decode requests. Numerous recent studies [3, 5, 12, 14, 31] propose a range of SLO-aware scheduling algorithms to improve SLO attainment.

PD Disaggregation Optimization. DistServe [46] proposes a PD-disaggregated architecture to entirely avoid interference between prefill and decode phases, which has since been widely adopted in modern inference engines like vLLM [32] and xLLM [20]. Subsequent research has further optimized this architecture from various angles, including parallelization strategies [46], KV cache management [25], and instance orchestration [33, 39]. Our scheduling algorithm is also designed to be effective in PD disaggregated settings.

Priority-related Request Scheduling. Existing request scheduling methods typically map request attributes, such as request length, SLO capability and online/offline nature, into priorities. Some methods [9, 11, 13, 38] treat shorter requests as higher priority, leveraging a scheduling strategy based on the Shortest Job First (SJF) principle. For instance, FastServe [38] introduces an enhanced multi-level priority queue, which dispatches incoming requests into different queue levels based on their prefill execution time. Studies [5, 31, 42] address multi-SLO scenarios by treating requests with tighter SLOs as higher priority. However, this scenario represents a subset of our context, as our approach not only accommodates heterogeneous request SLOs but also incorporates the priority of the client. Recent works [4, 30, 36] have proposed co-location scheduling for online and offline requests, typically prioritizing online requests as high-priority and offline requests as low-priority. They generally disregard the latency requirements of offline requests, making them unsuitable for direct application in our scenario. None of the aforementioned methods explicitly consider the inherent priority differences among online clients sending the requests. Llumnix [29] allocates more reserved memory space for high-priority requests. VTC [27] is a fairness-oriented scheduling algorithm. Its extension, Weighted VTC, introduces priority-specific weights to ensure that the ratio of processed tokens aligns with requests' priorities. However, relying solely on static token quotas or memory reservation cannot explicitly guarantee latency requirements of high-priority requests.

7 Conclusion

In this paper, we first formalize the multi-priority scheduling problem as a service gain maximization task, where meeting the latency requirements of high-priority requests typically yields greater service gain than satisfying those of low-priority requests. To address this, we propose PROSERVE, a novel scheduling framework consisting of: SlideBatching, the local scheduler, which adaptively reorders requests according to load and priority, and GoRouting, the global scheduler, which performs gain-oriented and capability-aware request dispatching across distributed instances. Extensive experiments across multiple datasets validate the effectiveness of our method.

References

[1] Amey Agrawal, Nitin Kedia, Ashish Panwar, Jayashree Mohan, Nipun Kwatra, Bhargav Gulavani, Alexey Tumanov, and Ramachandran Ramjee. Taming {Throughput-Latency} tradeoff in {LLM} inference with {Sarathi-Serve}. In *18th USENIX Symposium on Operating Systems Design and Implementation (OSDI 24)*, pages 117–134, 2024.

[2] Shuai Bai, Kebin Chen, Xuejing Liu, Jialin Wang, Wenbin Ge, Sibo Song, Kai Dang, Peng Wang, Shijie Wang, Jun Tang, et al. Qwen2. 5-vl technical report. *arXiv preprint arXiv:2502.13923*, 2025.

[3] Kyungmin Bin, Seungbeom Choi, Jimyoung Son, Jieun Choi, Daseul Bae, Daehyeon Baek, Kihyo Moon, Minsung Jang, and Hyojung Lee. Fineserve: Precision-aware kv slab and two-level scheduling for heterogeneous precision llm serving. *arXiv preprint arXiv:2509.06261*, 2025.

[4] Wan Borui, Zhao Juntao, Jiang Chenyu, Guo Chuanxiong, and Wu Chuan. Efficient llm serving on hybrid real-time and best-effort requests. *arXiv preprint arXiv:2504.09590*, 2025.

[5] Siyuan Chen, Zhipeng Jia, Samira Khan, Arvind Krishnamurthy, and Phillip B Gibbons. Slos-serve: Optimized serving of multi-slo llms. *arXiv preprint arXiv:2504.08784*, 2025.

[6] Tri Dao. Flashattention-2: Faster attention with better parallelism and work partitioning. *arXiv preprint arXiv:2307.08691*, 2023.

[7] Tri Dao, Dan Fu, Stefano Ermon, Atri Rudra, and Christopher Ré. Flashattention: Fast and memory-efficient exact attention with io-awareness. *Advances in neural information processing systems*, 35:16344–16359, 2022.

[8] Xianzhe Dong, Tongxuan Liu, Yuting Zeng, Liangyu Liu, Yang Liu, Siyu Wu, Yu Wu, Hailong Yang, Ke Zhang, and Jing Li. Hydrainfer: Hybrid disaggregated scheduling for multimodal large language model serving. *arXiv preprint arXiv:2505.12658*, 2025.

[9] Kuntai Du, Bowen Wang, Chen Zhang, Yiming Cheng, Qing Lan, Hejian Sang, Yihua Cheng, Jiayi Yao, Xiaoxuan Liu, Yifan Qiao, et al. Prefillonly: An inference engine for prefill-only workloads in large language model applications. In *Proceedings of the ACM SIGOPS 31st Symposium on Operating Systems Principles*, pages 399–414, 2025.

[10] Abhimanyu Dubey, Abhinav Jauhri, Abhinav Pandey, Abhishek Kadian, Ahmad Al-Dahle, Aiesha Letman, Akhil Mathur, Alan Schelten, Amy Yang, Angela Fan, et al. The llama 3 herd of models. *arXiv e-prints*, pages arXiv–2407, 2024.

[11] Yichao Fu, Siqi Zhu, Runlong Su, Aurick Qiao, Ion Stoica, and Hao Zhang. Efficient llm scheduling by learning to rank. *Advances in Neural Information Processing Systems*, 37:59006–59029, 2024.

[12] Ke Hong, Xiuhong Li, Lufang Chen, Qiuli Mao, Guohao Dai, Xuefei Ning, Shengen Yan, Yun Liang, and Yu Wang. Sola: Optimizing slo attainment for large language model serving with state-aware scheduling. In *Eighth Conference on Machine Learning and Systems*.

[13] Cunchen Hu, Heyang Huang, Liangliang Xu, Xusheng Chen, Jiang Xu, Shuang Chen, Hao Feng, Chenxi Wang, Sa Wang, Yungang Bao, et al. Inference without interference: Disaggregate llm inference for mixed downstream workloads. *arXiv preprint arXiv:2401.11181*, 2024.

[14] Jinqi Huang, Yi Xiong, Xuebing Yu, Wenjie Huang, Entong Li, Li Zeng, and Xin Chen. Slo-aware scheduling for large language model inferences. *arXiv preprint arXiv:2504.14966*, 2025.

[15] Sheng-Chun Kao, Suvinay Subramanian, Gaurav Agrawal, Amir Yazdanbakhsh, and Tushar Krishna. Flat: An optimized dataflow for mitigating attention bottlenecks. In *Proceedings of the 28th ACM International Conference on Architectural Support for Programming Languages and Operating Systems, Volume 2*, pages 295–310, 2023.

[16] Md Monjurul Karim, Sangeen Khan, Dong Hoang Van, Xinyue Liu, Chunhui Wang, and Qiang Qu. Transforming data annotation with ai agents: A review of architectures, reasoning, applications, and impact. *Future Internet*, 17(8):353, 2025.

[17] Woosuk Kwon, Zhuohan Li, Siyuan Zhuang, Ying Sheng, Lianmin Zheng, Cody Hao Yu, Joseph Gonzalez, Hao Zhang, and Ion Stoica. Efficient memory management for large language model serving with pagedattention. In *Proceedings of the 29th symposium on operating systems principles*, pages 611–626, 2023.

[18] Haoyang Li, Yiming Li, Anxin Tian, Tianhao Tang, Zhanchao Xu, Xuejia Chen, Nicole Hu, Wei Dong, Qing Li, and Lei Chen. A survey on large language model acceleration based on kv cache management. *arXiv preprint arXiv:2412.19442*, 2024.

[19] Aixin Liu, Bei Feng, Bing Xue, Bingxuan Wang, Bochao Wu, Chengda Lu, Chenggang Zhao, Chengqi Deng,

Chenyu Zhang, Chong Ruan, et al. Deepseek-v3 technical report. *arXiv preprint arXiv:2412.19437*, 2024.

[20] Tongxuan Liu, Tao Peng, Peijun Yang, Xiaoyang Zhao, Xiusheng Lu, Weizhe Huang, Zirui Liu, Xiaoyu Chen, Zhiwei Liang, Jun Xiong, et al. xllm technical report. *arXiv preprint arXiv:2510.14686*, 2025.

[21] Hongtao Lyu, Boyue Liu, Mingyu Wu, and Haibo Chen. Fairbatching: Fairness-aware batch formation for llm inference. *arXiv preprint arXiv:2510.14392*, 2025.

[22] NVIDIA. Dynamo. <https://github.com/ai-dynamo/dynamo>, 2025.

[23] OpenAI. Introducing chatgpt. <https://openai.com/index/chatgpt/>, 2022.

[24] Chandandeep Singh Pabla. Completely fair scheduler. *Linux Journal*, 2009(184):4, 2009.

[25] Ruoyu Qin, Zheming Li, Weiran He, Jialei Cui, Heyi Tang, Feng Ren, Teng Ma, Shangming Cai, Yineng Zhang, Mingxing Zhang, et al. Mooncake: A kvcache-centric disaggregated architecture for llm serving. *ACM Transactions on Storage*, 2024.

[26] ShareGPT. Sharegpt. https://huggingface.co/datasets/anon8231489123/ShareGPT_Vicuna_unfiltered, 2023.

[27] Ying Sheng, Shiyi Cao, Dacheng Li, Banghua Zhu, Zhuohan Li, Danyang Zhuo, Joseph E Gonzalez, and Ion Stoica. Fairness in serving large language models. In *18th USENIX Symposium on Operating Systems Design and Implementation (OSDI 24)*, pages 965–988, 2024.

[28] Jovan Stojkovic, Chaojie Zhang, Íñigo Goiri, Josep Torrellas, and Esha Choukse. Dynamollm: Designing llm inference clusters for performance and energy efficiency. In *2025 IEEE International Symposium on High Performance Computer Architecture (HPCA)*, pages 1348–1362. IEEE, 2025.

[29] Biao Sun, Ziming Huang, Hanyu Zhao, Wencong Xiao, Xinyi Zhang, Yong Li, and Wei Lin. Llumnix: Dynamic scheduling for large language model serving. In *18th USENIX symposium on operating systems design and implementation (OSDI 24)*, pages 173–191, 2024.

[30] Ting Sun, Penghan Wang, and Fan Lai. Hygen: Efficient llm serving via elastic online-offline request co-location. *arXiv preprint arXiv:2501.14808*, 2025.

[31] Yinghao Tang, Tingfeng Lan, Xiuqi Huang, Hui Lu, and Wei Chen. Scorpio: Serving the right requests at the right time for heterogeneous slos in llm inference. *arXiv preprint arXiv:2505.23022*, 2025.

[32] vLLM Team. vllm. <https://github.com/vllm-project/vllm>, 2025.

[33] Chao Wang, Pengfei Zuo, Zhangyu Chen, Yunkai Liang, Zhou Yu, and Ming-Chang Yang. Prefill-decode aggregation or disaggregation? unifying both for goodput-optimized llm serving. *arXiv preprint arXiv:2508.01989*, 2025.

[34] Jiahao Wang, Jinbo Han, Xingda Wei, Sijie Shen, Dingyan Zhang, Chenguang Fang, Rong Chen, Wenyuan Yu, and Haibo Chen. Kvcache cache in the wild: Characterizing and optimizing kvcache cache at a large cloud provider, 2025.

[35] Yuxin Wang, Yuhuan Chen, Zeyu Li, Xueze Kang, Yuchu Fang, Yeju Zhou, Yang Zheng, Zhenheng Tang, Xin He, Rui Guo, et al. Burstgpt: A real-world workload dataset to optimize llm serving systems. In *Proceedings of the 31st ACM SIGKDD Conference on Knowledge Discovery and Data Mining V. 2*, pages 5831–5841, 2025.

[36] Zhibin Wang, Shipeng Li, Xue Li, Yuhang Zhou, Zhonghui Zhang, Zibo Wang, Rong Gu, Chen Tian, Kun Yang, and Sheng Zhong. Echo: Efficient co-scheduling of hybrid online-offline tasks for large language model serving. *arXiv preprint arXiv:2504.03651*, 2025.

[37] Zhibin Wang, Shipeng Li, Yuhang Zhou, Xue Li, Rong Gu, Nguyen Cam-Tu, Chen Tian, and Sheng Zhong. Revisiting slo and goodput metrics in llm serving. *arXiv preprint arXiv:2410.14257*, 2024.

[38] Bingyang Wu, Yinmin Zhong, Zili Zhang, Shengyu Liu, Fangyue Liu, Yuanhang Sun, Gang Huang, Xuanzhe Liu, and Xin Jin. Fast distributed inference serving for large language models. *arXiv preprint arXiv:2305.05920*, 2023.

[39] Yu Wu, Tongxuan Liu, Yuting Zeng, Siyu Wu, Jun Xiong, Xianzhe Dong, Hailong Yang, Ke Zhang, and Jing Li. Arrow: Adaptive scheduling mechanisms for disaggregated llm inference architecture. *arXiv preprint arXiv:2505.11916*, 2025.

[40] xLLM Team. xllm. <https://github.com/jd-opensource/xllm>, 2025.

[41] An Yang, Anfeng Li, Baosong Yang, Beichen Zhang, Binyuan Hui, Bo Zheng, Bowen Yu, Chang Gao, Chen-gen Huang, Chenxu Lv, et al. Qwen3 technical report. *arXiv preprint arXiv:2505.09388*, 2025.

[42] Zahra Yousefijamarani, Xinglu Wang, Qian Wang, Morgan Lindsay Heisler, Taha Shabani, Niloofar Gholipour, Parham Yassini, Hong Chang, Kan Chen, Qiantao Zhang, et al. Hyperflexis: Joint design of algorithms and systems for multi-slo serving and fast scaling. *arXiv preprint arXiv:2508.15919*, 2025.

- [43] Jintao Zhang, Jia Wei, Haofeng Huang, Pingle Zhang, Jun Zhu, and Jianfei Chen. Sageattention: Accurate 8-bit attention for plug-and-play inference acceleration. *arXiv preprint arXiv:2410.02367*, 2024.
- [44] Wei Zhang, Zhiyu Wu, Yi Mu, Banruo Liu, Myungjin Lee, and Fan Lai. Tempo: Application-aware llm serving with mixed slo requirements. *arXiv preprint arXiv:2504.20068*, 2025.
- [45] Lianmin Zheng, Liangsheng Yin, Zhiqiang Xie, Chuyue Livia Sun, Jeff Huang, Cody Hao Yu, Shiyi Cao, Christos Kozyrakis, Ion Stoica, Joseph E Gonzalez, et al. Sclang: Efficient execution of structured language model programs. *Advances in neural information processing systems*, 37:62557–62583, 2024.
- [46] Yinmin Zhong, Shengyu Liu, Junda Chen, Jianbo Hu, Yibo Zhu, Xuanzhe Liu, Xin Jin, and Hao Zhang. {DistServe}: Disaggregating prefill and decoding for goodput-optimized large language model serving. In *18th USENIX Symposium on Operating Systems Design and Implementation (OSDI 24)*, pages 193–210, 2024.